LE STUDIUM

CONFERENCES

Challenges and opportunities in materials for green energy production and conversion

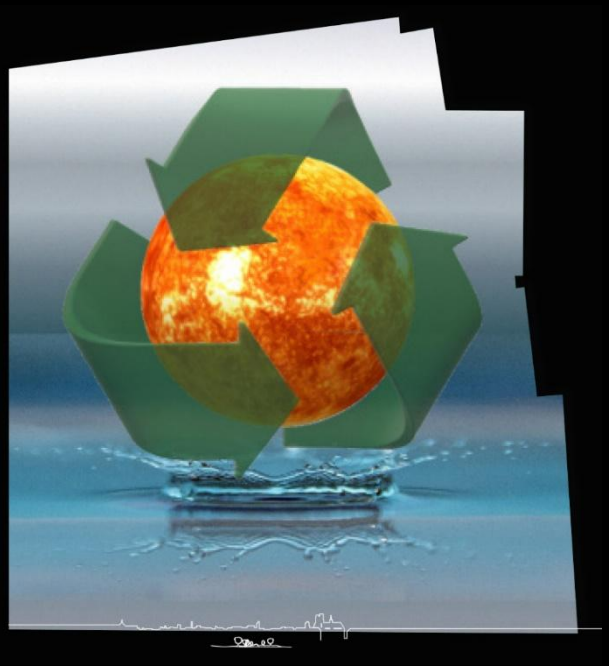

THURSDAY 17th June 2021 – 15:10

Dr. Pascal Brault

Groupe de Recherches sur l'Energétique des Milieux Ionisés, CNRS Université d'Orléans, Orléans – FR

"Reactive molecular dynamics simulations of H2 production and conversion"

Outline

- Practical MD simulations
- Green hydrogen production
  - H_2O reactivity with Aluminum
  - Biomass in Supercritical water and pyrolysis (not so green)
- H_2 conversion in low temperature fuel cells
  - Supported and free nanocatalyst growth
  - Oxygen Reduction Reaction
- Conclusions

Practical Molecular Dynamics simulation

- ✓ Calculate all trajectories of a set of atoms, molecules, ...
  via the Newton equation of motion
  → Suitable for processes at nanoscale (up to 10^9 atoms)

- ✓ A rigourous approach requires the use of robust interaction potentials
  If necessary running DFT, i.e. electronic calculations → *ab-initio* or *first-principles* MD and/or Machine Learning methods

- ✓ and initial conditions (positions, velocities) preferably matching experimental conditions
  → appropriate velocity distribution functions can be derived from experimental conditions.

- ✓ Proper energy dissipation:
  - Energy release during deposition, bond formation/breaking
  - Annealing

  → via friction term(s), thermostat(s)

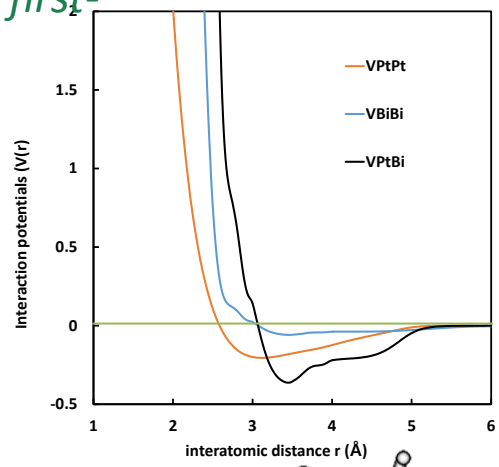

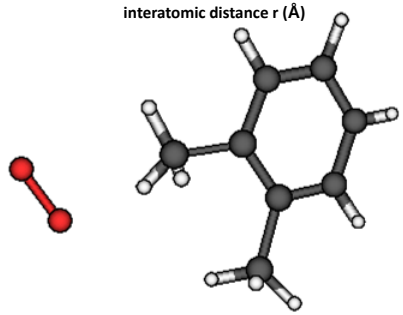

Practical Molecular Dynamics simulation

Relevance/significance of MD Simulations

Flux :

Exp. 1 $10^{15} cm^{-2} s^{-1}$ = 10 species / nm^2 / s - MD 1 specie /10x10 nm^2 / 2 ps

Prohibit long time diffusion, except if including specific strategies (fbMC, CVHD, hyperdynamics, …)

Pressure/simulation box size

Solid density : Pt 65 nm^{-3} Liquid density: water 33 nm^{-3}

If box size is in the range 10 x 10 x 10 nm^3 → 65 000 Pt atoms or 33 000 water molecules

→ Statistical quantities (diffusion coeff, reaction rates, etc) can be directly calculated

Gas density : 1 atm = 2.4 10^{-2} nm^{-3}

-> Not enough species in box of size d at pressure P

→ Chemistry and reactivity in the gas phase require scaling law between simulation box and reactor sizes

Solution: relevant parameter = Collision number $\propto$ P.d → ↑P ↓d should work.

Practical Molecular Dynamics simulation

1/ recovering/scaling experimental conditions

Hypothesis : Collision number are the same in experiments and simulations so, $P_{exp} d_{exp} = P_{sim} d_{sim}$ thus $N_{sim} = \frac{P_{exp}}{k_B T_g} \cdot S_{sim} \cdot d_{exp}$ and if r_{cut} is the largest cutoff radius : $d_{sim} > \frac{N_{sim}}{S_{sim}} \cdot {r_{cut}}^3$

Or equivalently $\rho_{sim} = \frac{N_{sim}}{V_{sim}} < \frac{1}{r_{cut}^3}$

(S_{sim}, V_{sim} are the chosen smallest area, volume of the simulation box)

2/ Experimental time recovery

→ Velocities are same in experiments and simulations

$$v = \frac{d_{exp}}{t_{exp}} = \frac{d_{sim}}{t_{sim}}, when\ d_{exp}, d_{sim} > 2\rho$$

$$then, t_{exp} = \frac{d_{exp}}{d_{sim}} . t_{sim}, when\ d_{exp}, d_{sim} > 2\rho$$

$$or, t_{exp} = t_{sim}, when\ d_{exp}, d_{sim} \leq 2\rho$$

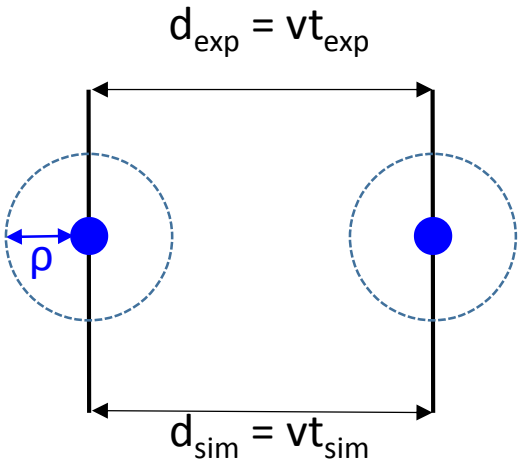

P. Brault, *Multiscale Molecular Dynamics Simulation of Plasma Processing: Application to Plasma Sputtering*, Front. Phys. 6 (2018) 59

Practical Molecular Dynamics simulation

Thermal relaxation

- Choose a relevant specie release time: i.e. greater than thermalisation time
- Choose a relevant thermostat (region i.e. which should be thermostated) within this relevant time
- For interactions with surface, one can guess that only the substrate should be thermostated

Practical Molecular Dynamics simulation Interaction potentials

New reactive and including electron interaction potentials (force fields) allow targeting multiscale MD simulations

2/ combine improved force fields

Plasma factor	Possible?	Example
electric field	yes	CNT growth
atoms and hyperthermal species	yes	Si-NW oxidation
radicals	yes	a-C:H growth
ions	yes	sputtering
electronically excited states	yes	etching
vibrationally excited states	yes / no (reaxFF)	/
photons	implicit	(polymer degradation)
electrons	Yes (eFF, e-reaxFF)	/

E. Neyts, P. Brault (Review article), *Molecular dynamics simulations for plasma surface interactions*, Plasma Processes and Polymers 14 (2017) 1600145

Practical Molecular Dynamics simulation: Interactions potentials

Metals : Embedded Atom Method (EAM) (well suited for metal catalysts)

⇒ energy of a solid is a unique functional of the electron density.

⇒ uses the concept of electron (charge) density to describe metallic bonding:

⇒ each atom contributes through a spherical, exponentially-decaying field of electron charge, centered at its nucleus, to the overall charge density of the system.

⇒ Binding of atoms is modelled as embedding these atoms in this “pool” of charge, where the energy gained by embedding an atom at location r is some function of the local density.

⇒ The total energy thus writes:

With pairwise function:

and mixing rule:

S.M. Foiles, M.I. Baskes Contributions of the embedded-atom method to materials science and engineering, MRS Bulletin, 37 (2012) 485-491.
X. W. Zhou et al, Misfit-energy-increasing dislocations in vapor-deposited CoFe/NiFe multilayers, Phys. Rev. B 69 (2004) 144113

Practical Molecular Dynamics simulation: Interactions potentials

ReaxFF allows for computationally efficient simulation of materials under realistic conditions, *i.e.* bond breaking and formation with accurate chemical energies. It also includes variable partial charges.

Due to the chemistry, ReaxFF has a complicated potential energy function: $E_{system} = E_{bond} + E_{over} + E_{angle} + E_{tors} + E_{vdWaals} + E_{Coulomb} + E_{Specific}$

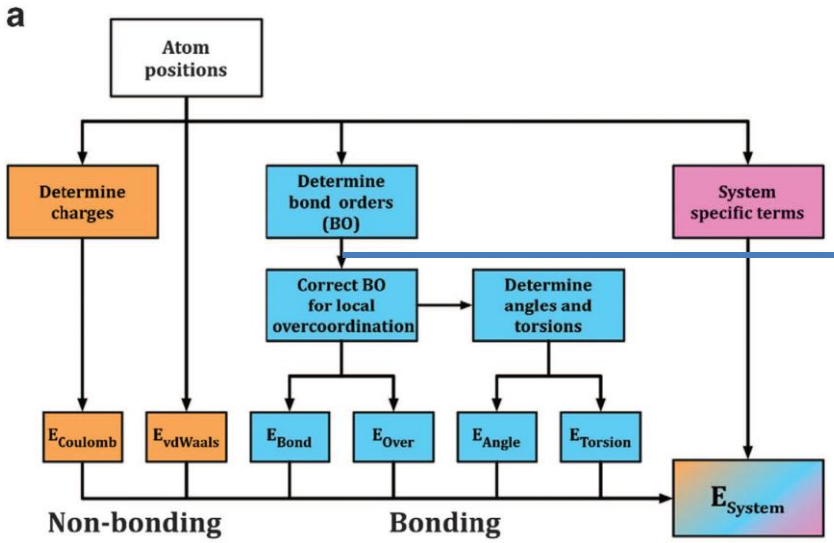

Overview of the ReaxFF total energy components

$$BO_{ij} = BO_{ij}^{\sigma} + BO_{ij}^{\pi} + BO_{ij}^{\pi\pi}$$
$$= \exp\left[p_{bo1}\left(\frac{r_{ij}}{r_o^{\sigma}}\right)^{p_{bo2}}\right] + \exp\left[p_{bo3}\left(\frac{r_{ij}}{r_o^{\pi}}\right)^{p_{bo4}}\right]$$
$$+ \exp\left[p_{bo5}\left(\frac{r_{ij}}{r_o^{\pi\pi}}\right)^{p_{bo6}}\right]$$

Correct Bond Order ⇒ Correct description of reaction energy barriers

Parametrization using experimenatal known data and DFT calculations

TP Senftle et al, *The ReaxFF reactive force-field: development, applications and future directions*, npj Computational Materials 2, (2016) 15011

H_2 production: Al-H_2O

- Basically:

$$2Al_{(s)} + 6H_2O_{(l)} \rightarrow 3H_{2(g)} + 2Al(OH)_{3(aq)} + Q_1 \quad (1)$$

$$2Al_{(s)} + 4H_2O_{(l)} \rightarrow 3H_{2(g)} + 2AlOOH_{(aq)} + Q_2 \quad (2)$$

$$2Al_{(s)} + 3H_2O_{(l)} \rightarrow 3H_{2(g)} + Al_2O_{3(aq)} + Q_3 \quad (3)$$

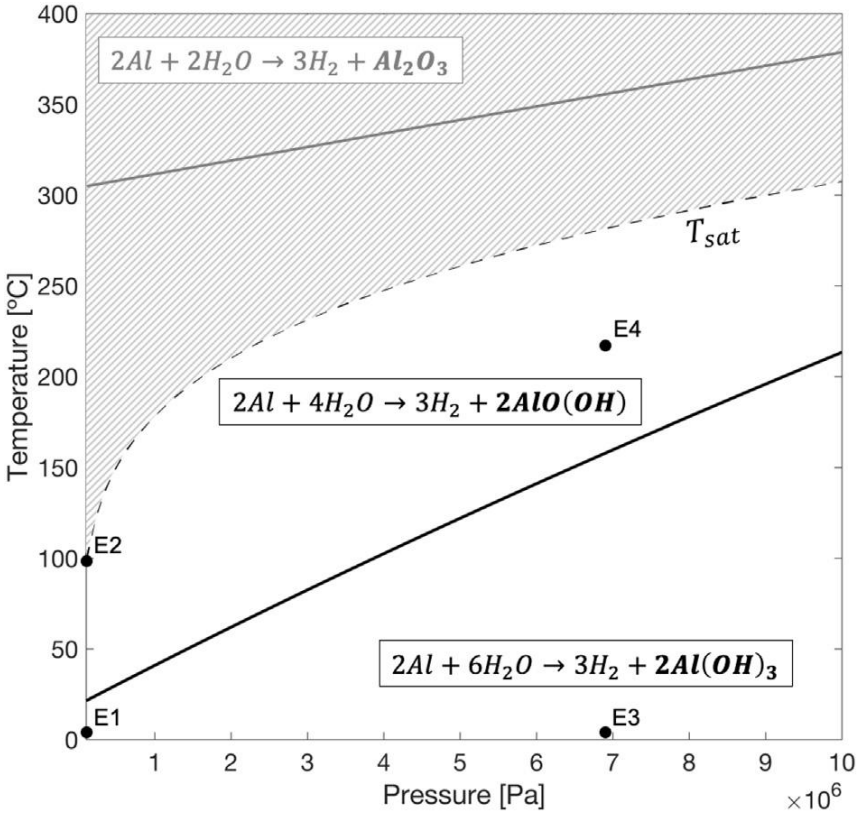

P. Godart et al, Hydrogen production from aluminum-water reactions subject to varied pressures and temperatures, *Int. J. Hydrogen Energy* 44 (2019) 11448 -11458

H.Z. Wang et al, A review on hydrogen production using aluminum and aluminum alloys, *Renewable and Sustainable Energy Reviews* **13** (2009) 845–853

H_2 production: Al-H_2O

- A reaxFF forcefield has been specially designed for H_2O interactions with Al

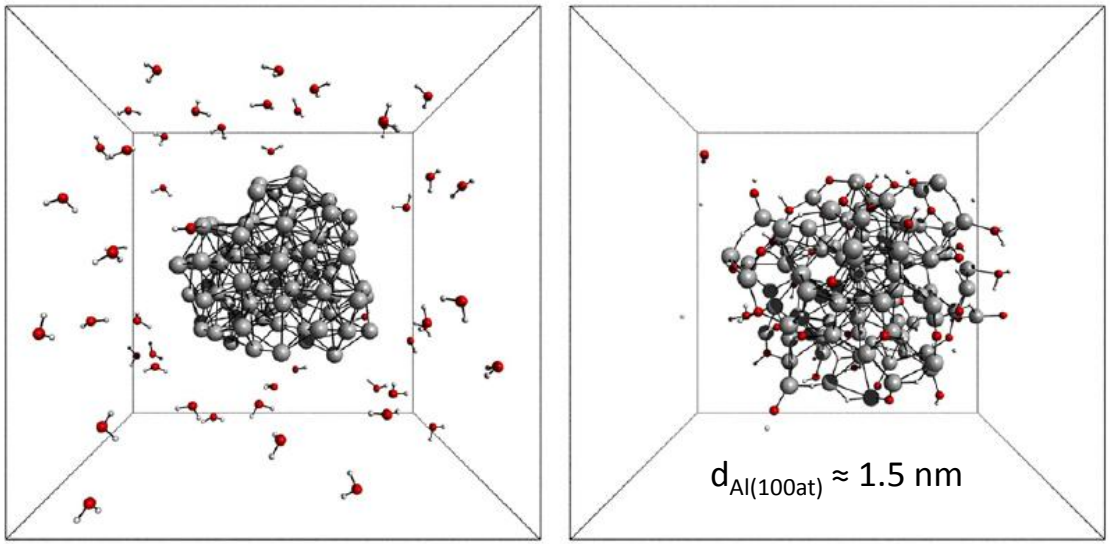

Fig. 1 – Images of the initial (left, 0 ps) and final (right, 66 ps) configuration of the Al_{100} cluster with $50H_2O$ molecules.

Table 4 – Summary of the simulation cases involving oxygen molecules.

Simulation case	H_2O (g)	H_2O (ads)	H_2O (dis)	H_2 (g)	H (ads)	OH (ads)	O (ads)
$Al_{100}\cdot 50(H_2O)$	1	7	42	1	52	30	0
$Al_{100}\cdot 25(O_2)\cdot 50(H_2O)$	11	13	26	1	17	26	40
$Al_{100}\cdot 50(O_2)\cdot 50(H_2O)$	25	7	36	3	2	17	62
$Al_{100}\cdot 79(O_2)\cdot 50(H_2O)$	41	0	9	0	0	2	72

M. F. Russo et al, Molecular dynamic simulation of aluminum-water reactions using the ReaxFF reactive force field, *Int. J. Hydrogen Energy* 44 (2019) 11448 -11458

H_2 production: Al-H_2O

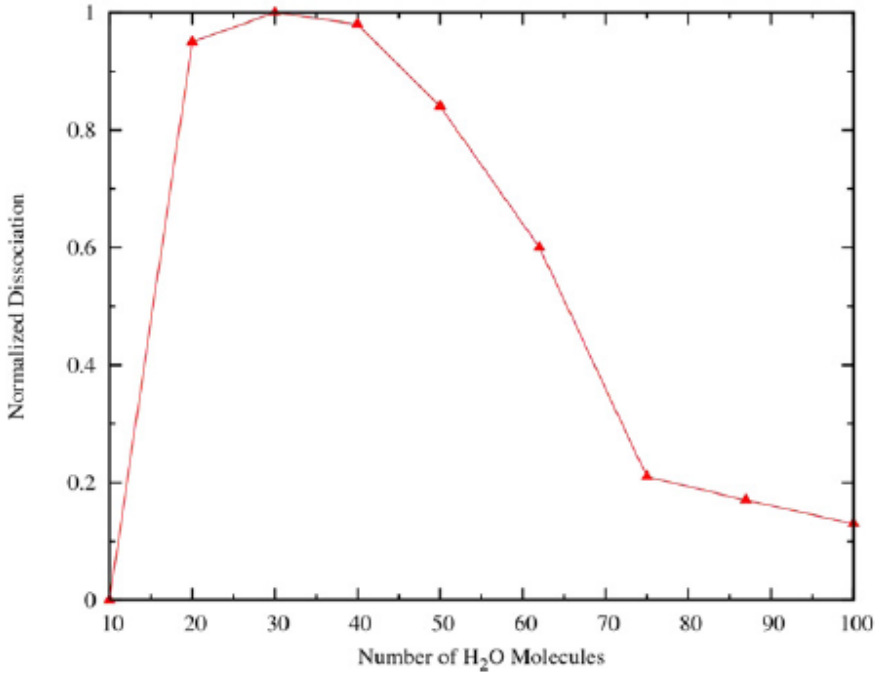

Fig. 6 – The water dissociation completion percentage as a function of initial amount of water used on an Al_{100} cluster. We observe a maximum dissociation at 30 water molecules, providing an optimal balance between catalytic waters and surface site availability.

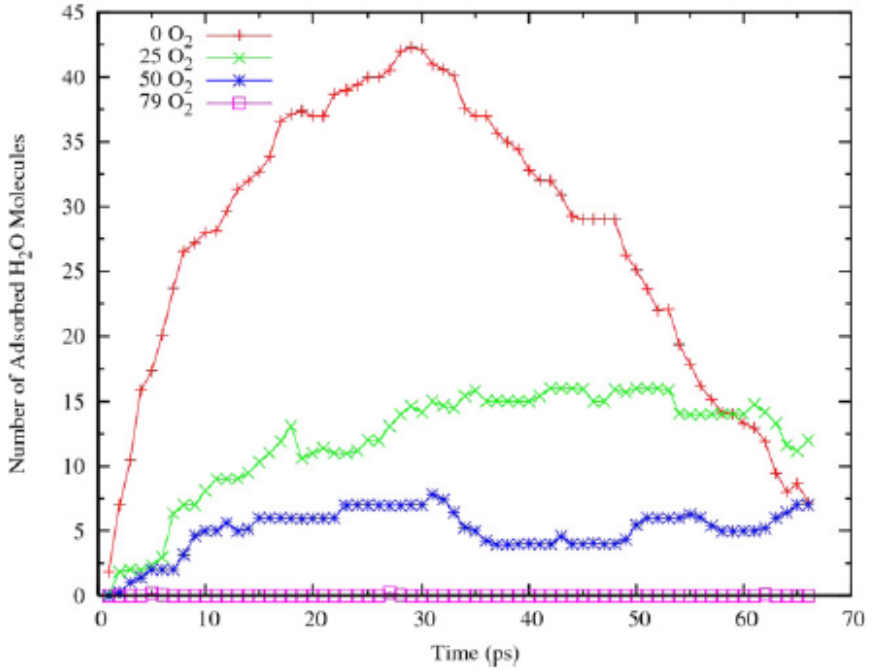

Fig. 8 – The number of adsorbed water molecules on the Al_{100} surface as a function of time in the presence of 25, 50, or 79 O_2 molecules.

- Water self-poisoning
- Adding O_2

H_2 production: Al-H_2O

- Ab-initio Molecular Dynamics

  PWA approximation, GGA exchange – correlation electronic calculation (-> forcefield) at each time step + dynamics using MD

  But 400h calculation on 64 processors for 6 ps duration at 1000K

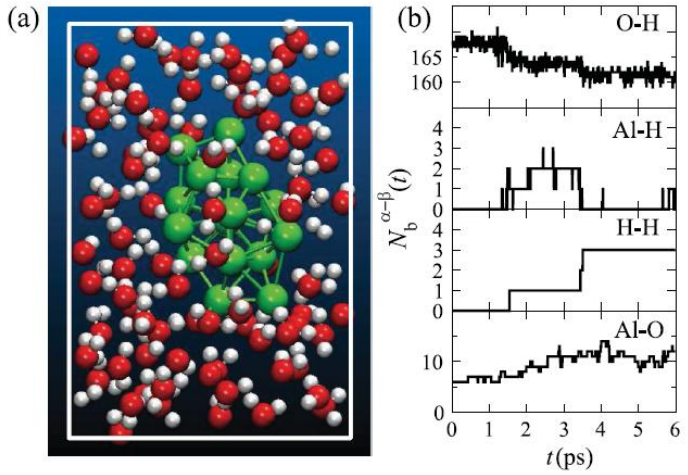

FIG. 1 (color). (a) Snapshot of the Al_{17} + water system, where green, red, and white spheres represent aluminum, oxygen, and hydrogen atoms, respectively. (b) Time evolution of the number of chemical bonds $N_b^{\alpha-\beta}(t)$. Two atoms are considered bonded when their distance is less than a cutoff distance R_c during a prescribed bond lifetime 12 fs [16], where R_c is 1.3, 2.0, 1.0, and 2.4 Å for O-H, Al-H, H-H, and Al-O pairs, respectively.

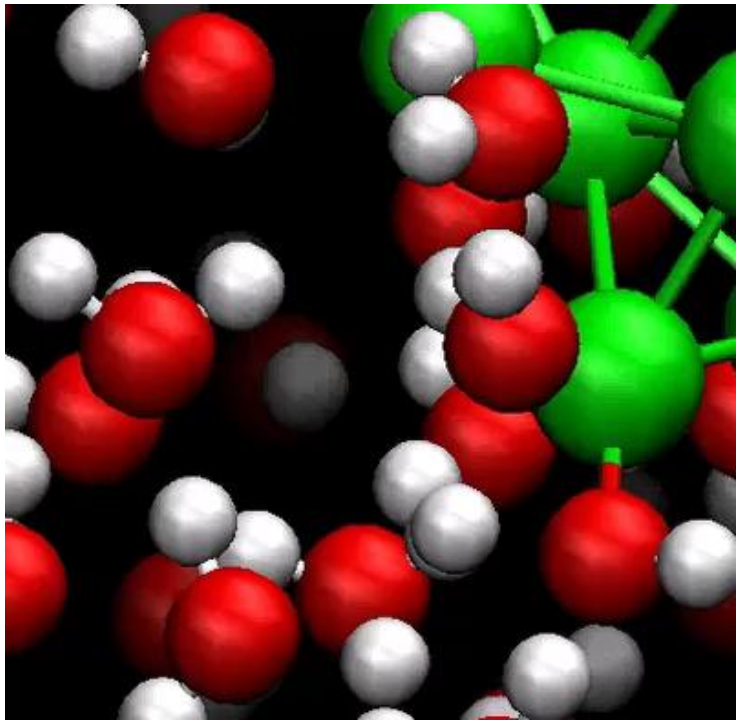

F. Shimoro et al, Molecular Dynamics Simulations of Rapid Hydrogen Production from Water Using Aluminum Clusters as Catalyzers, *Phys. Rev. Lett.* 104 (2010) 126102

H_2 Production: Biomass in SCW

- Combining DFT and ReaxFF MD for coal (not biomass) conversion in SCW

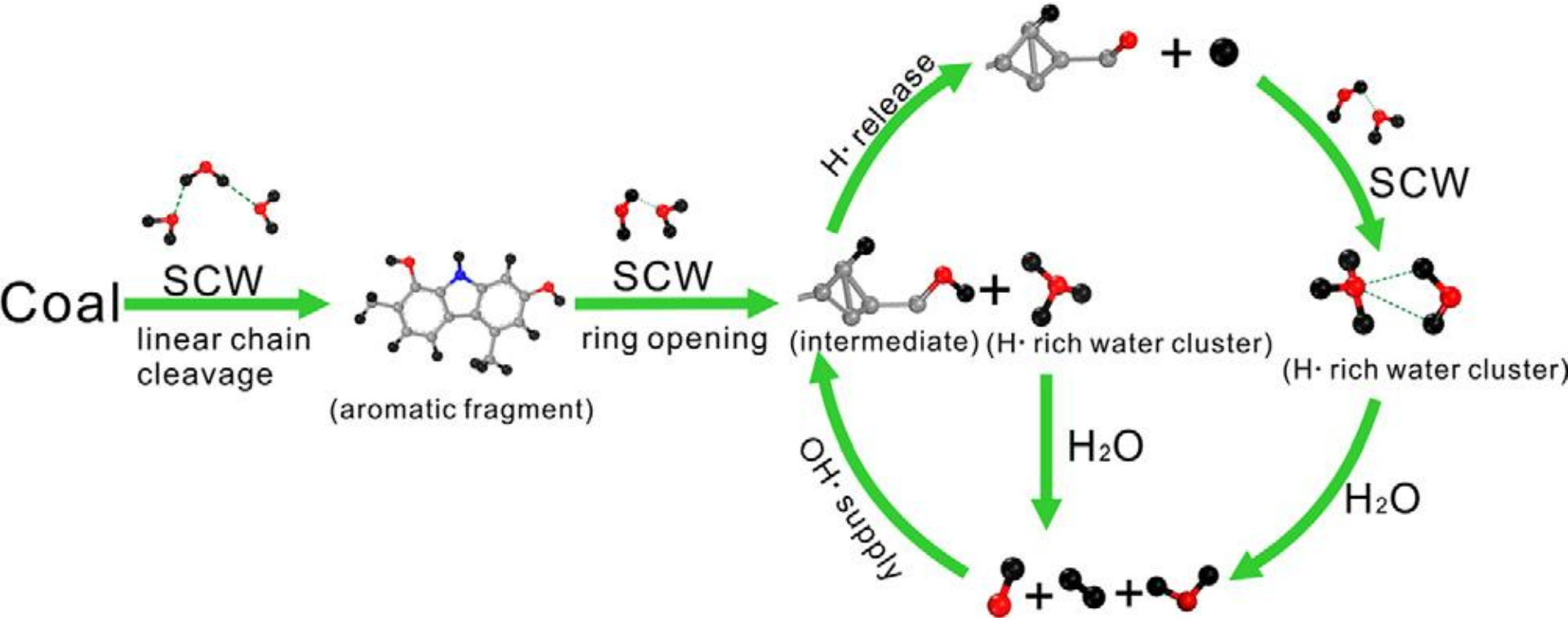

J. Zhang et al , The effect of supercritical water on coal pyrolysis and hydrogen production: A combined ReaxFF and DFT study, Fuel 108 (2013) 682–690

H_2 Production: Biomass in SCW

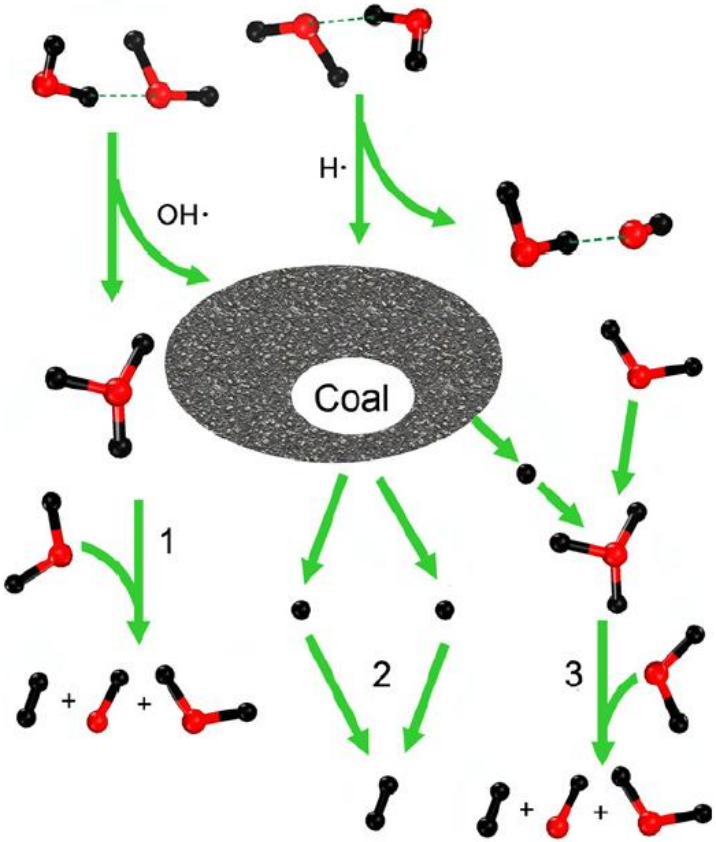

Fig. 7. Three reaction paths for H_2 production in the SCW–coal system.

H_2 Production: Biomass pyrolysis

- ReaxFF MD simulations
  - → 1 biomass molecule and 1000H_2O + 200 O_2)in a (100Å)^3 box
  - → T = 1000, 1500, 1800, and 2000 K

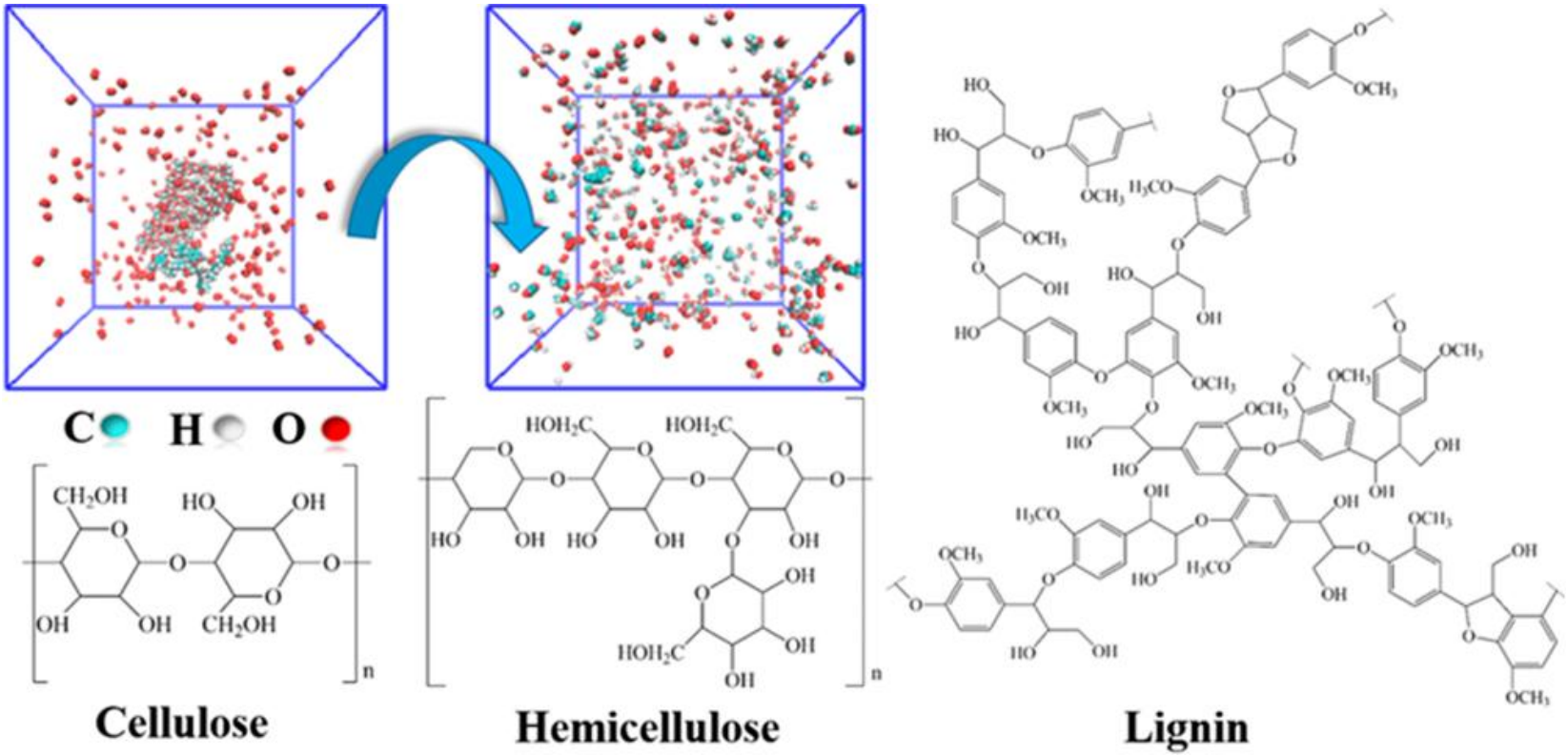

C. Chen et al, Reactive Molecular Dynamics Simulations of Biomass Pyrolysis and Combustion under Various Oxidative and Humidity Environments, Ind. Eng. Chem. Res. 56 (2017) 12276-12288

H_2 Production: Biomass pyrolysis

- Lignin pyrolysis is providing the highest H_2 ratio

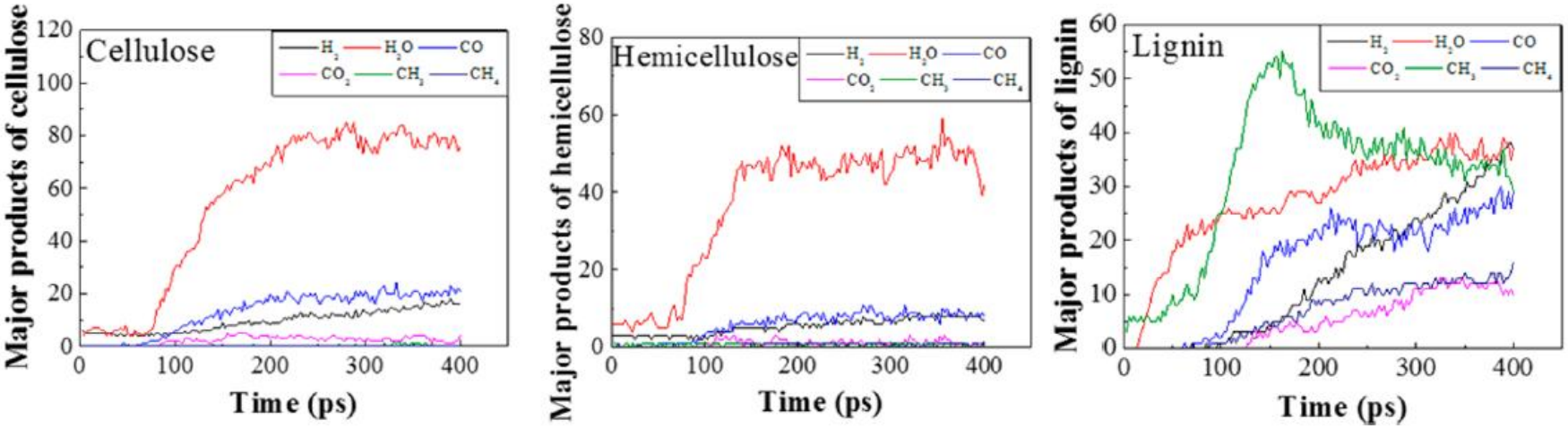

Figure 3. Time evolution (in number of molecules) of major pyrolysis products of cellulose, hemicellulose, and lignin at 2000 K.

H_2 conversion in low temperature fuel cells : Supported and free nanocatalyst growth

- Supported Pt_2PdAu nanocatalyst growth on porous carbon: Sequential PdAu deposition followed by Pt deposition

Potentials used in the system:
Pt-Pd-Au: EAM potentials
C – C: Tersoff potential -> thermostat
Metal – C: LJ potential (Steele)
Model porous carbon from TEM measurements

→ $AuPd@Pt_2$ core@shell
But always Au segregation towards surface!

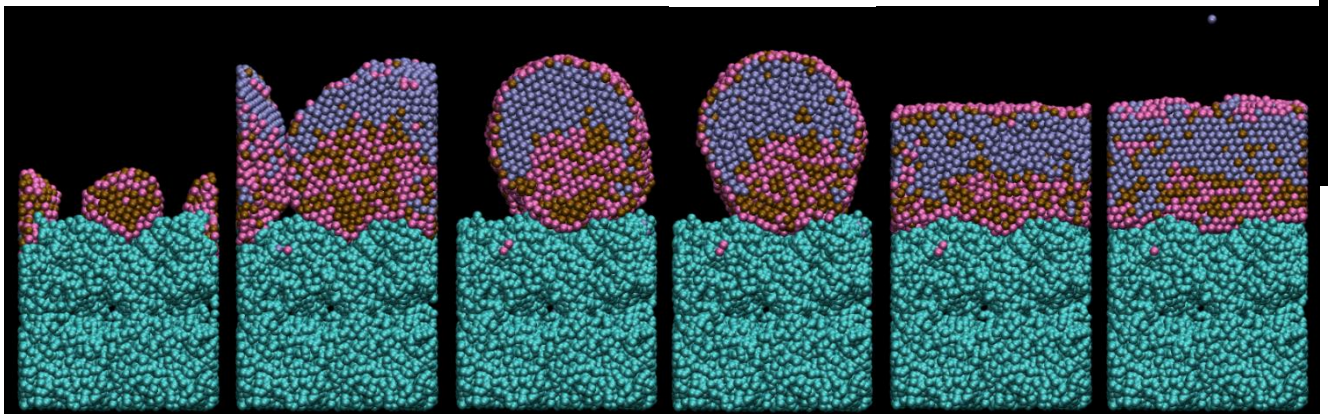

• Pt; • Pd; • Au

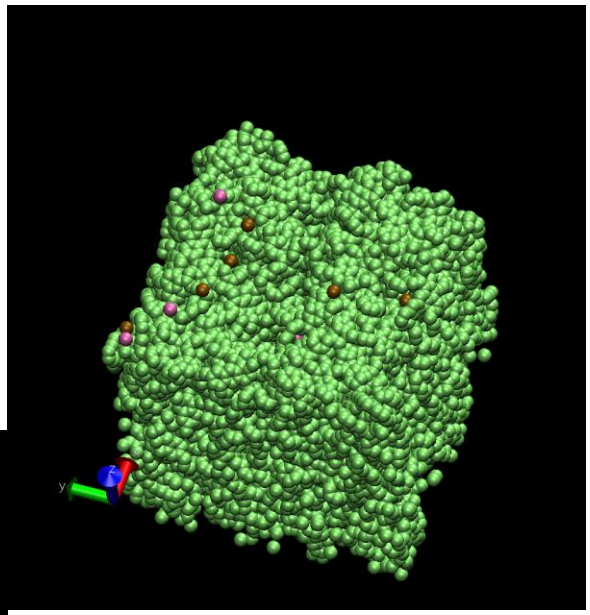

Table 1 – EAM and average experimental surface energies of the low index faces of Pt, Pd, Au in Jm^{-2} [40].			
	Pt	Pd	Au
(111)	1.44	1.22	0.79
(100)	1.65	1.37	0.92
(110)	1.75	1.49	0.98
Experimental, face averaged	2.49	2.00	1.5

P. Brault, Molecular dynamics simulations of ternary PtxPdyAuz fuel cell nanocatalyst growth, International Journal of Hydrogen Energy 41 (2016) 22589-22597

H_2 conversion in low temperature fuel cells : Supported and free nanocatalyst growth

Correlations between cluster temperature evolution and morphology transform in the course of deposition of core-shell PdAu@Pt_2 nanocatalyst

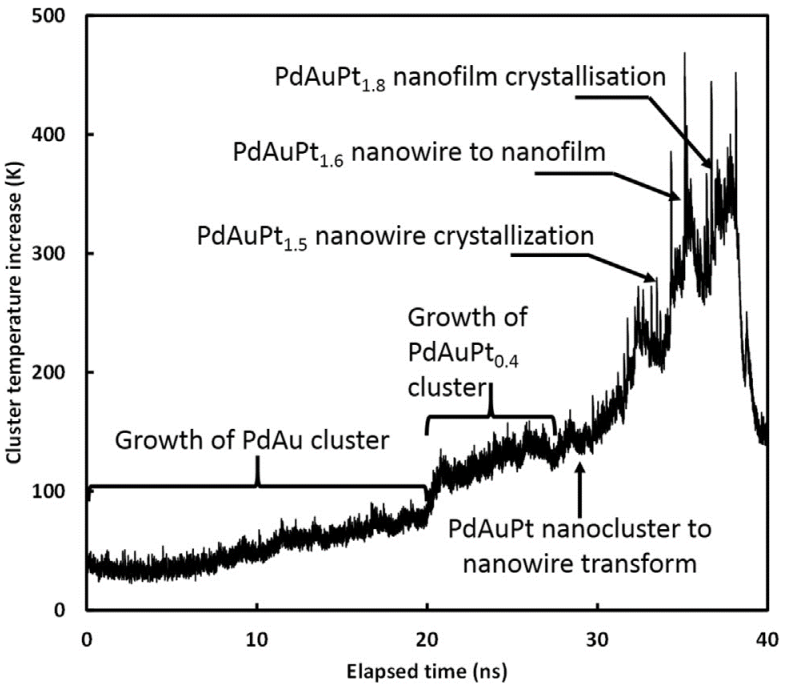

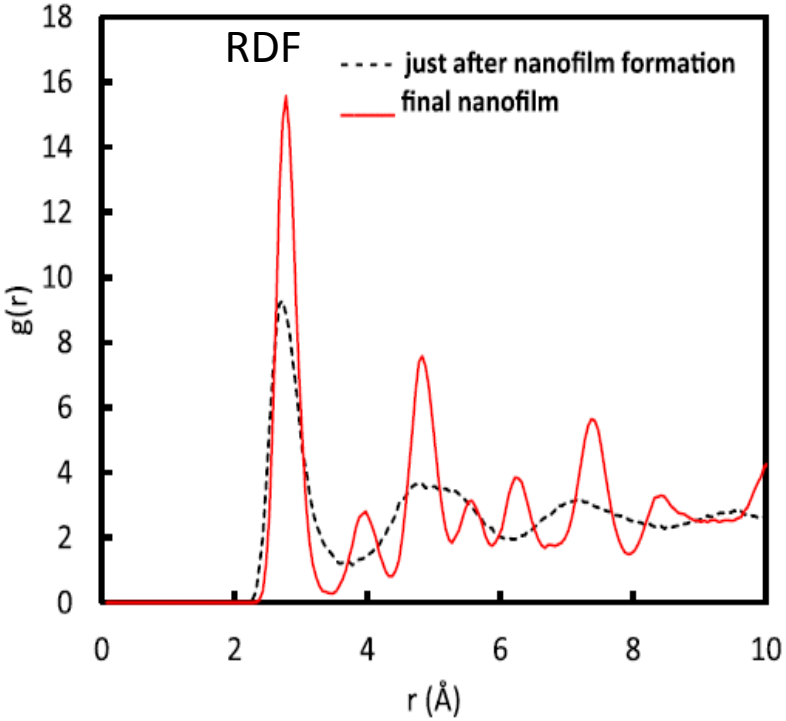

- L. Xie, P. Brault, C. Coutanceau, A. Caillard, J. Berndt, E. Neyts Appl. Cat. B, 62 (2015) 21 – 26
- P. Brault, et al, International Journal of Hydrogen Energy 41 (2016) 22589-22597
- E. Neyts, P. Brault, Plasma Processes and Polymers 14 (2017) 1600145 - FP7 FCH-JU SMARTCat project #325327

H_2 conversion in low temperature fuel cells : Supported and free nanocatalyst growth

- Free $Pt_3Me(Au)$ (Me = Ni, Cu) nanocatalyst growth

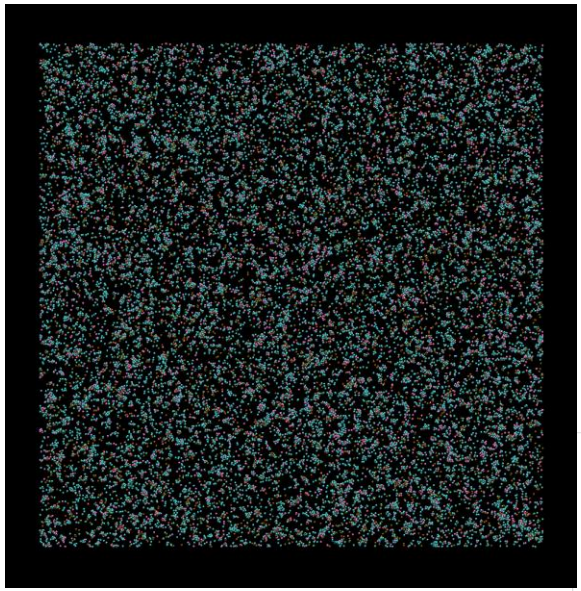

Tricks :

NVE ensemble for Pt, Ni and Au

NVT ensemble for Ar : surrounding gas is the thermostat

Ratio of N_{Ar} to N_{metal} estimated from experiments: depends on discharge current, Ar pressure, …

here: N_{Ar}=128000; N_{Pt}=19200; N_{Ni}=6400; N_{Au}=6400

Box size 64x64x64 nm^3; dt = 1 fs, 4. 10^7 timesteps

Temperature evolution of the vapor and of the metal vapor and then of clusters the →cluster growth and coalescence : breaks in the plot (green vertical sticks)

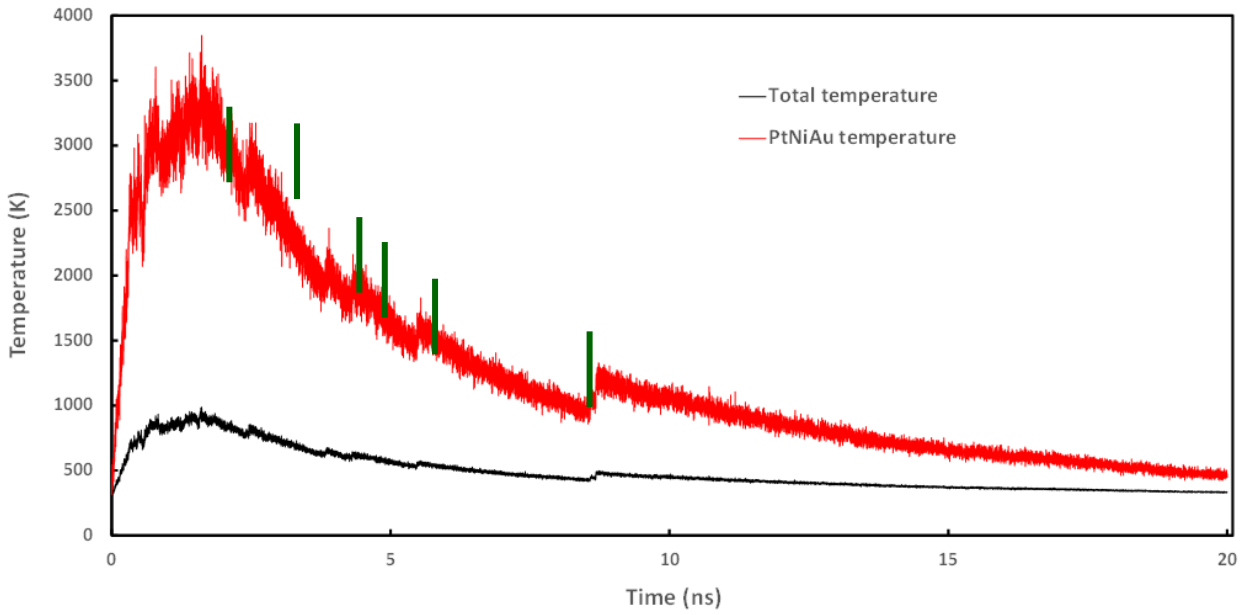

H_2 conversion in low temperature fuel cells : Supported and free nanocatalyst growth

- Free $Pt_3Me(Au)$ (Me = Ni, Cu) nanocatalyst growth

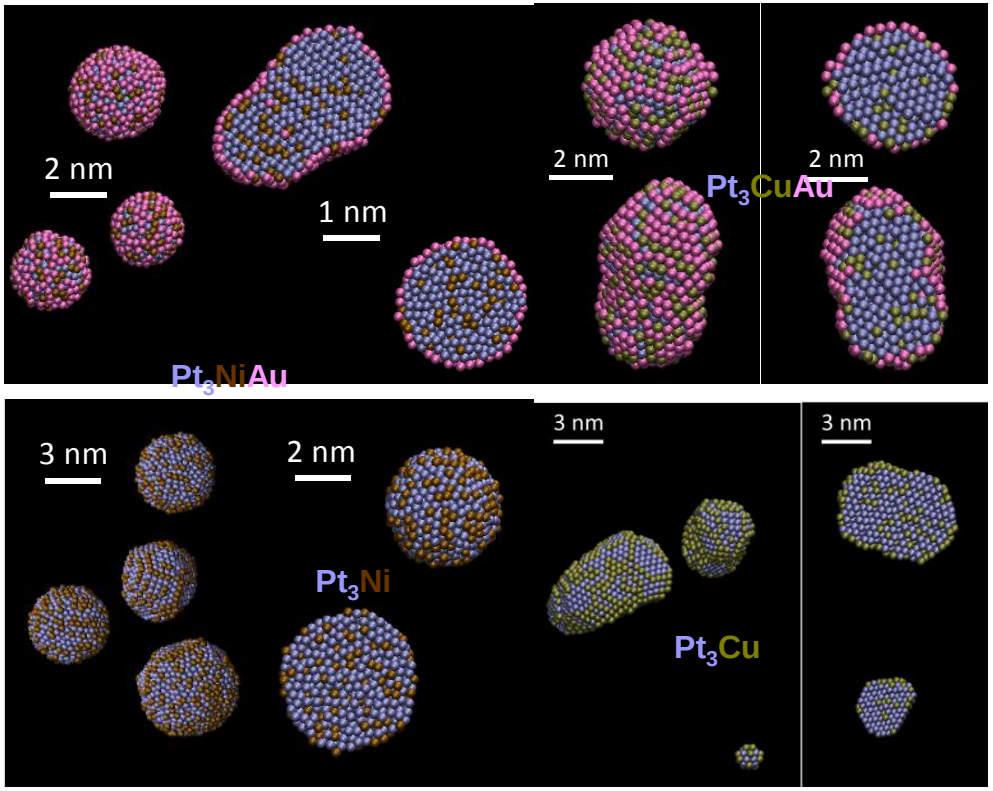

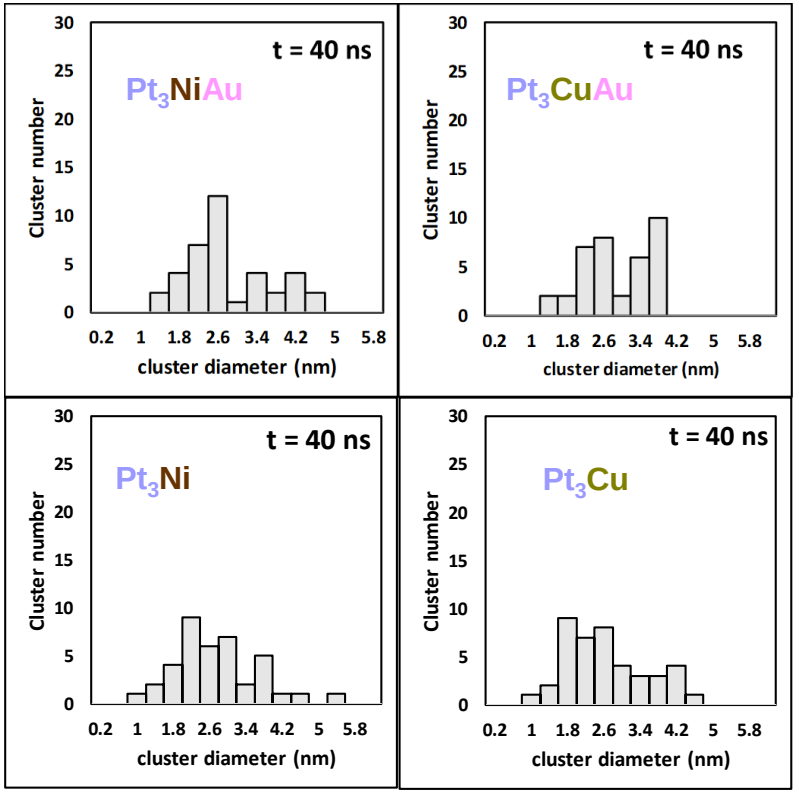

- Au segregation towards cluster surface
- CuAu surface alloy for Pt_3CuAu → better efficiency for Oxygen Reduction Reaction as observed
- $Pt_3Cu(Au)$ more well crystallized

P. Brault et al, Pt_3MeAu (Me = Ni, Cu) fuel cell nanocatalyst growth, shapes and efficiency: A molecular dynamics simulation approach, J. Phys. Chem. C 123 (2019) 29656

H_2 conversion in low temperature fuel cells : Supported and free nanocatalyst growth

- Pt_xBi_y nanocatalyst growth

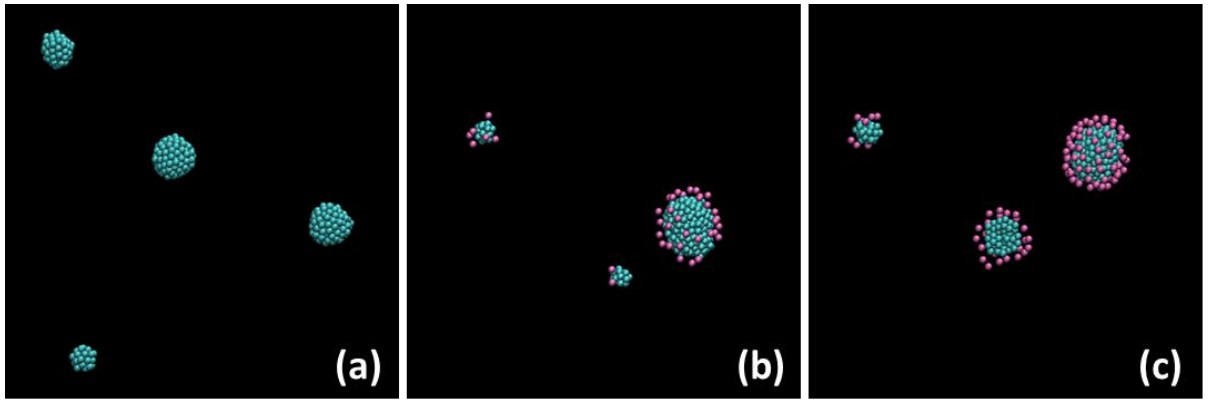

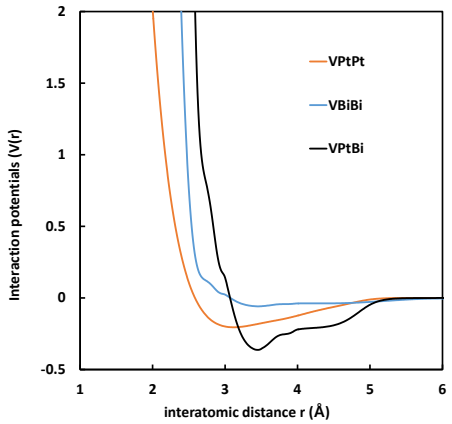

Snapshot of the final clusters at 20 ns. Argon atoms (4000) are not represented for clarity. $n_{Pt} + n_{Bi} = 500$. (a) Pt alone (b) Pt_9Bi_1 (c) Pt_8Bi_2. Box size 16x16x16 nm^3

Plots of the pair part of the EAM interaction potentials: $V_{PtPt}(r)$, $V_{BiBi}(r)$, $V_{PtBi}(r)$.

- Cluster atomic arrangements are typical of a crystalline structure of the Pt cores, with numbers of 1st nearest neighbors between 10 and 12 (i.e. consistent with fcc arrangement)
- Bi composition < 20% leads to cluster surfaces with both Pt and Bi, allowing catalytic activity enhancement.
- Pt/Bi atomic composition is not only globally preserved, but is also verified for each cluster

B.S.R. Kouamé et al, Insights on the unique electro-catalytic behavior of PtBi/C materials, *Electrochimica Acta* 329 (2020) 135161

H_2 conversion in low temperature fuel cells: Oxygen Reduction Reaction

- PEM Fuel Cell

anode $H_2 \rightarrow 2H^+ + 2e^-$

$C_xH_yO + (2x-1)H_2O \xrightarrow[\text{Catalyst}]{} xCO_2 + (5x-2)H^+ + (5x-2)e^-$

$2H^+ + 1/2\ O_2 + 2e^- \xrightarrow[\text{Catalyst}]{} H_2O$ *Cathode ORR*

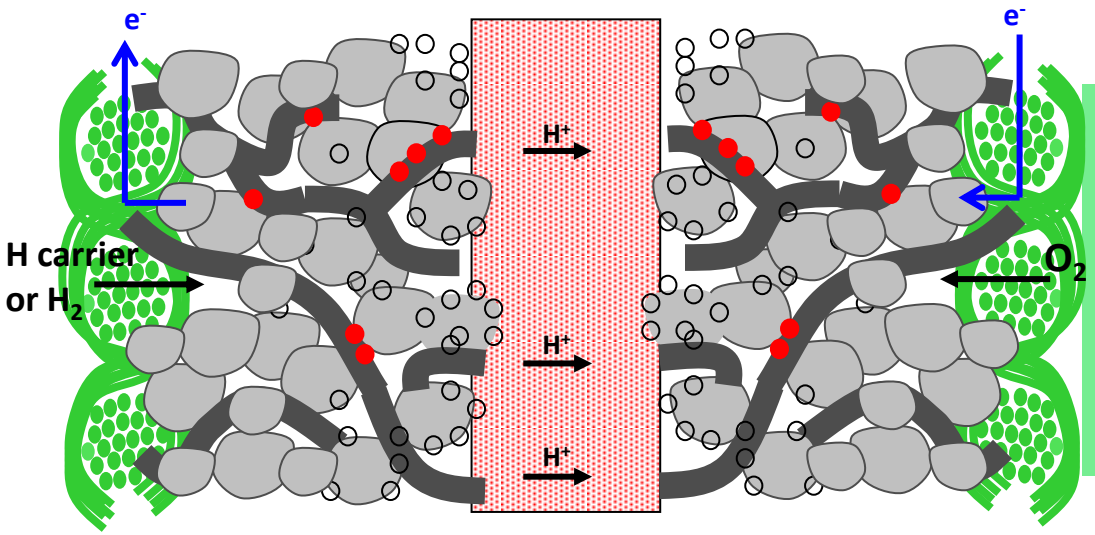

THREE PHASE BOUNDARY

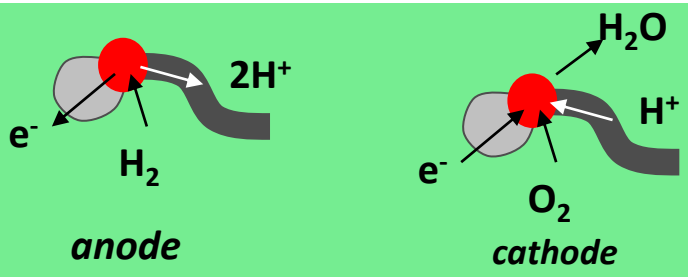

Catalyst +Electrolyte + Conducting material are required simultaneously for the reactions

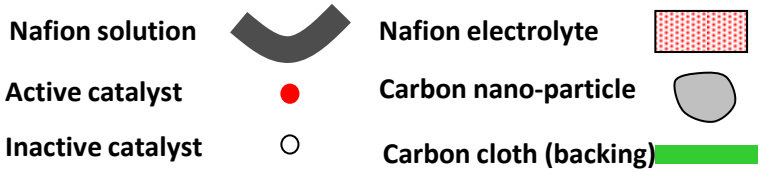

H_2 conversion in low temperature fuel cells: Oxygen Reduction Reaction

- A « realistic » three phase bounadry:
  water + Nafion electrolyte + Pt nanocatalyst supported on graphite

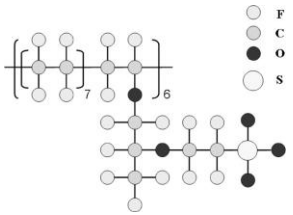

Nafion© monomer

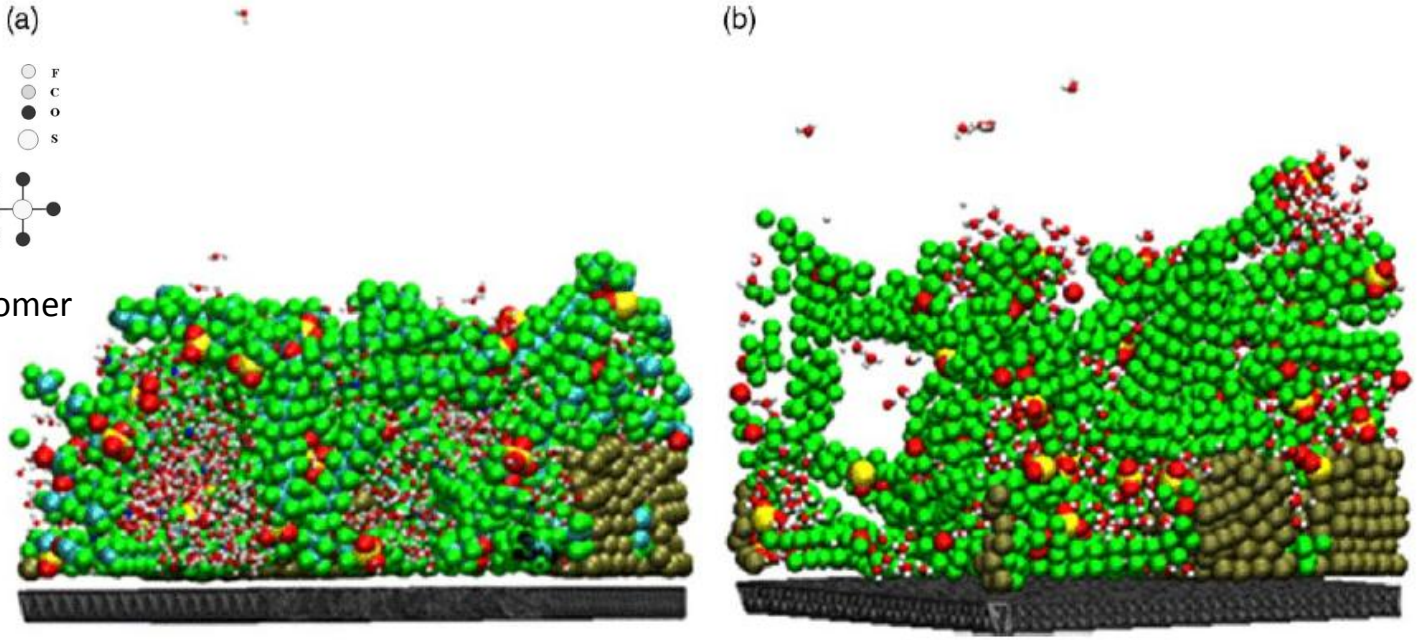

Fig. 1. Side view of the system at the simulated maximum NAFION content (14 NAFION-4, and $\lambda = 24$). Water clustering is observed near the sulfonic groups and the model NAFION layer totally covering the catalyst particles. (a) Well-packed NAFION structure obtained from deposition without annealing procedure. (b) Alternative model where NAFION has been partially detached after an annealing procedure. Color coding for the figure is as follows: F, green; O, red; H, white; S, yellow; Pt, tan; C, cyan (not visible in the pictures since it is covered by the F atoms) and the graphite layer is represented by the two parallel planes shown at the bottom. (For interpretation of the references to color in this figure legend, the reader is referred to the web version of the article.)

E. J. Lamas et al, Molecular dynamics studies of a model polymer–catalyst–carbon interface, Electrochimica Acta 51 (2006) 5904–5911

H_2 conversion in low temperature fuel cells: Oxygen Reduction Reaction

- Oxygen transport through the electrolyte

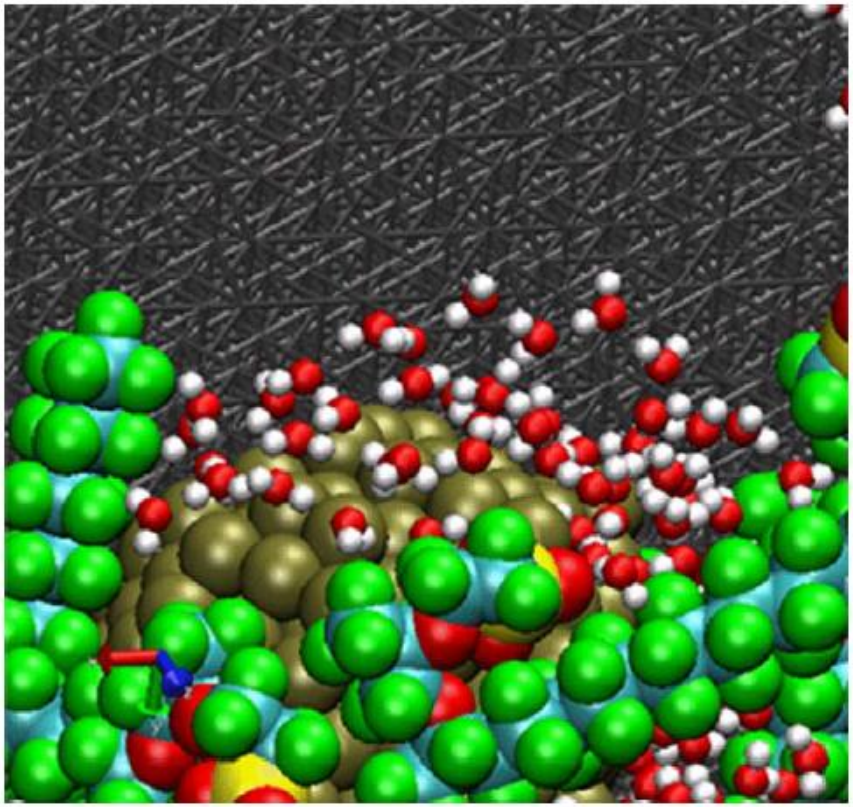

Fig. 5. Details of the interface catalyst surface/water/model NAFION (for a polymer content of 7 NAFION-4/cell, $\lambda = 24$). Notice water organization over the catalyst surface.

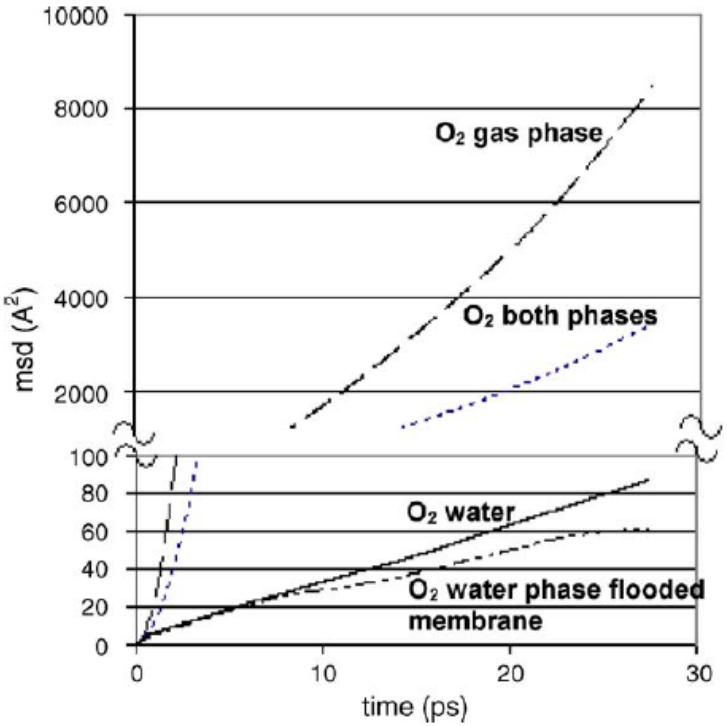

Fig. 7. Time evolution of the O_2 mean square displacement, providing estimates of O_2 diffusion in water at the conditions of flooded NAFION ($\lambda = 64$). O_2 diffusion in pure water is provided as a reference. Notice that oxygen diffusion in the flooded MEA gives values close to the ones calculated for bulk water but deviating at long times because of the absence of an Einstein type diffusion mechanism in the MEA.

H_2 conversion in low temperature fuel cells: Oxygen Reduction Reaction

- Effects of Pt nanocatalyst size

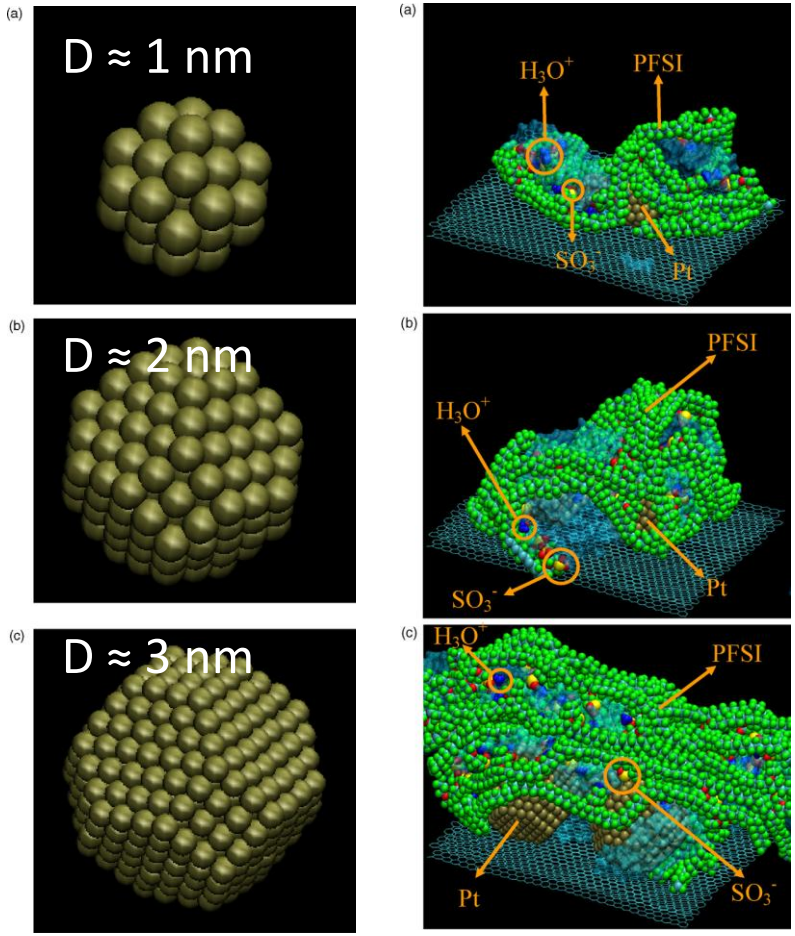

Initial and final configuration of the supported Pt nanocatlyst under three phase boundary interaction

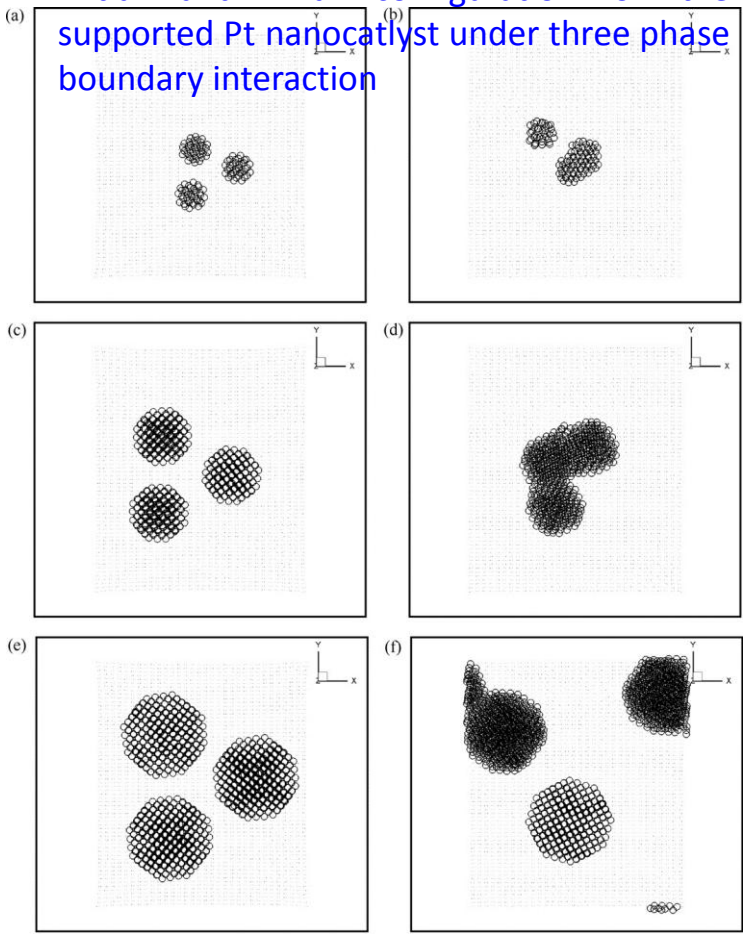

C.H. Cheng et al, Effect of Pt nano-particle size on the microstructure of PEM fuel cell catalyst layers: Insights from molecular dynamics simulations, Electrochimica Acta 55 (2010) 1588–1597

H_2 conversion in low temperature fuel cells: Oxygen Reduction Reaction

- Ab-initio molecular dynamics of the ORR

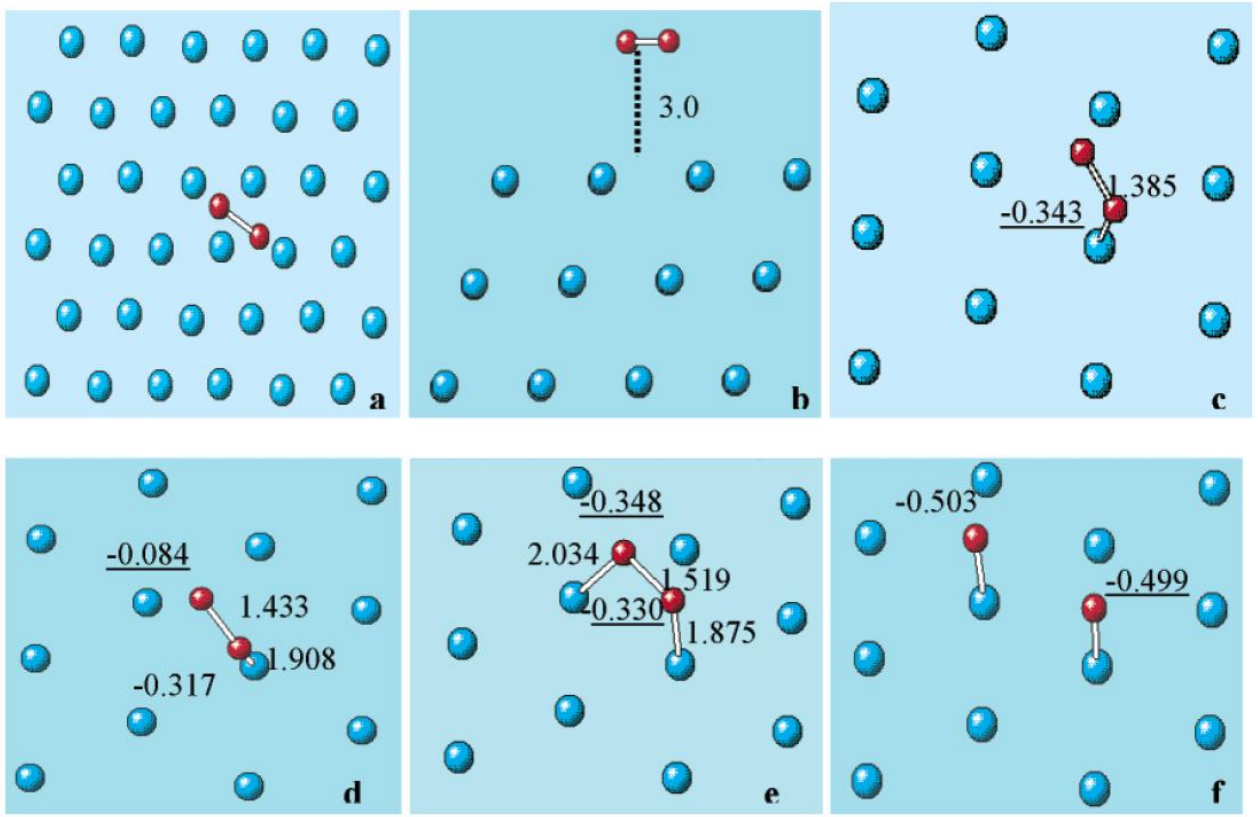

Figure 1. Snapshots of the O_2 + Pt(111) trajectory at 350 K. Only the surface layer is included in Figures (c)−(f) for clarity. The underlined data refers to the charge carried by adjacent oxygen atoms. (a) Top view of the initial configuration wherein O_2 is located parallel (3.0 Å above) to the Pt(111) surface, over the 2-fold bridge site. (b) Side view of the initial configuration. (c) One-end chemisorbed precursor at 0.24 ps, in which one oxygen is chemisorbed atop the Pt atom (at 1.85 Å) while the other oxygen is still far (2.80 Å) from the surface, and R_{O-O} = 1.38 Å. (d) One-end chemisorbed precursor at 0.36 ps, with distances oxygen−surface R_{O-S} = 2.47 and 1.91 Å, and R_{O-O} = 1.43 Å. (e) Top−bridge−top intermediate at 0.41 ps, with R_{O-S} = 1.87 and 2.03 Å and R_{O-O} = 1.52 Å. (f) Atop atomic adsorption at 1.16 ps.

Y. Wang and P. B. Balbuena, Roles of Proton and Electric Field in the Electroreduction of O2 on Pt(111) Surfaces: Results of an Ab-Initio Molecular Dynamics Study, J. Phys. Chem. B **108** (2004) 4376-4384

H_2 conversion in low temperature fuel cells: Oxygen Reduction Reaction

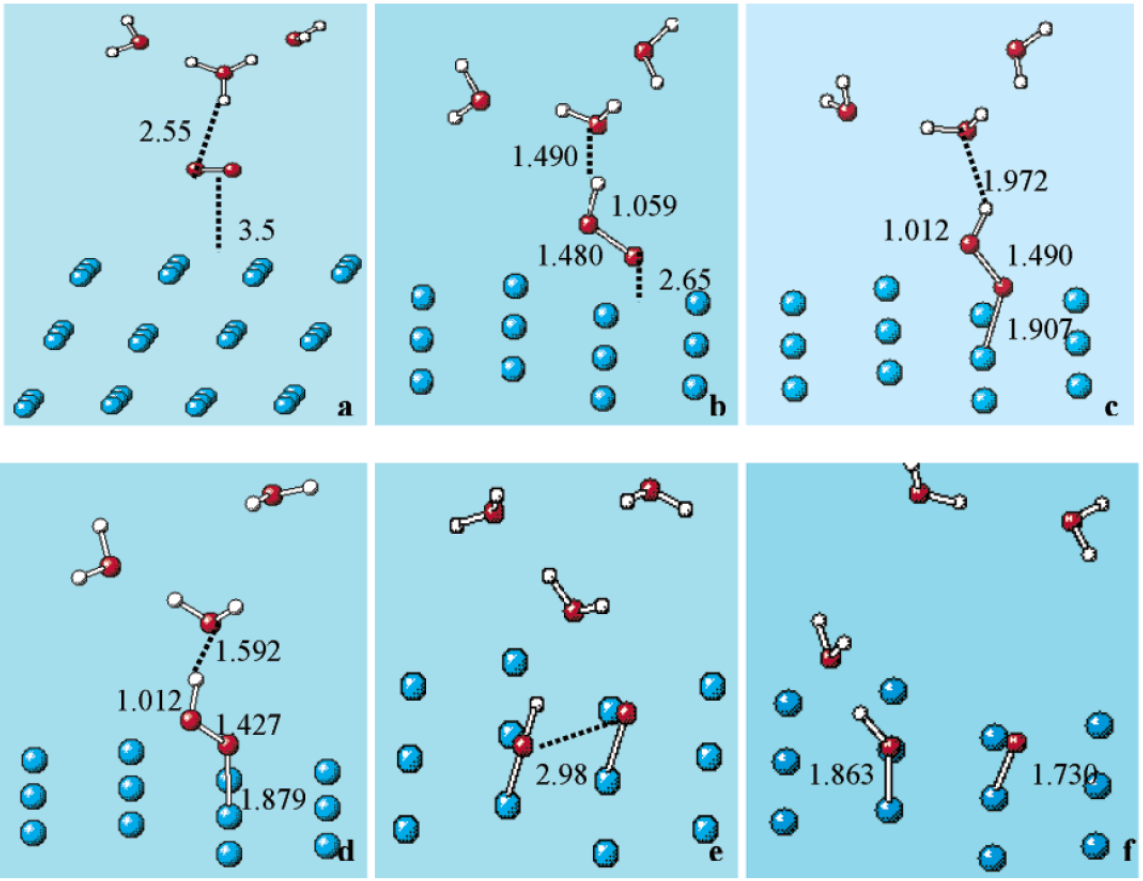

Figure 3. Snapshots of the $O_2 + H^+(H_2O)_3$/Pt(111) trajectory at 350 K. For clarity, only the surface layer is included in 3(b)−(f). (a) Side view of the initial configuration wherein O_2 is located parallel (3.5 Å above) to the Pt(111) surface, over the 2-fold bridge site, and the proton is separated from O_2 by 2.55 Å. (b) Formation of the proton-transfer intermediate $H^+-O-O\cdots Pt$ at 0.25 ps. (c) One-end chemisorbed precursor $H^+-O-O-Pt$ at 0.30 ps, wherein a strong interaction exists between the oxygen end and the Pt(111) surface, evidenced by the short distance R_{O-s} = 1.91 Å. (d) Another view of the one-end chemisorbed precursor at 0.42 ps. (e) Dissociation of the one-end chemisorbed precursor and consequent chemisorption of OH at 0.50 ps. (f) The chemisorbed hydroxyl in atop site at 0.85 ps.

H_2 conversion in low temperature fuel cells: Oxygen Reduction Reaction

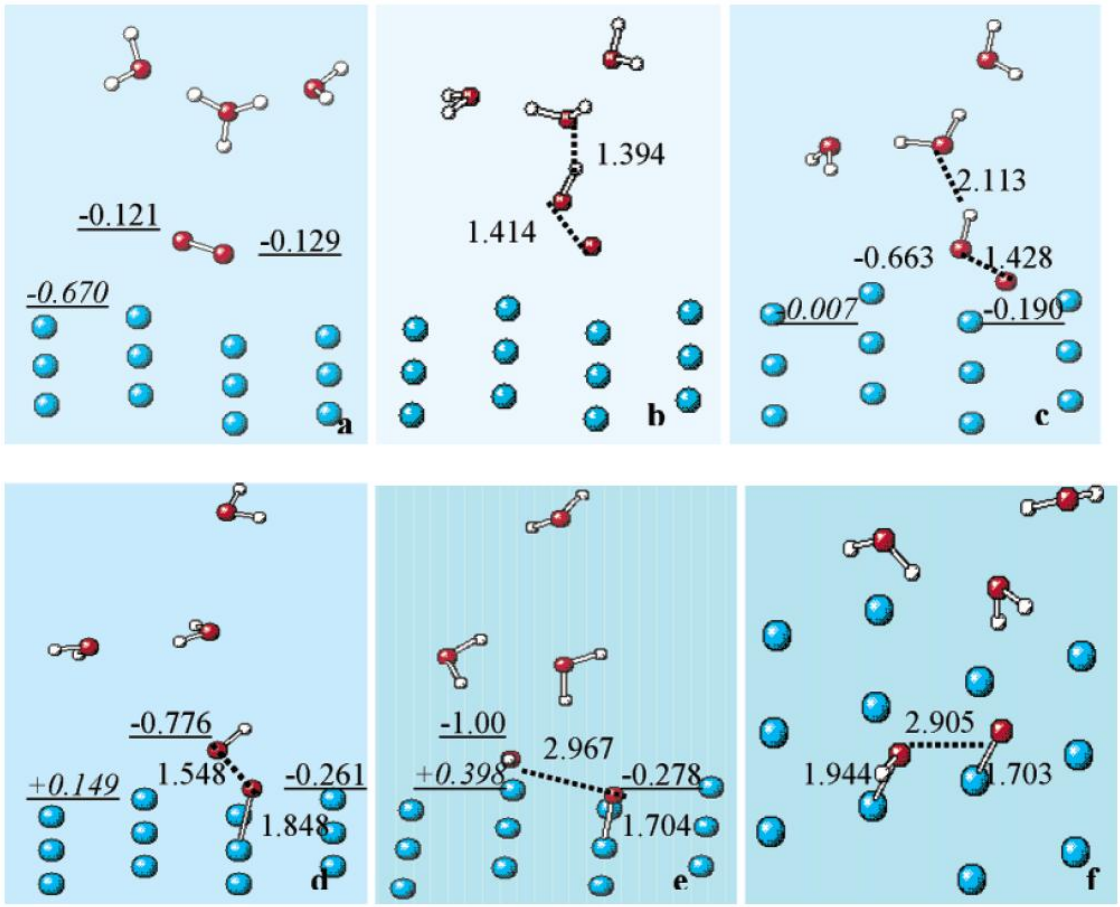

Figure 6. Snapshots of the $O_2 + H^+(H_2O)_3 + e^-/Pt(111)$ system at 350 K. For clarity, only the surface layer is included. The underlined data refers to the charge carried by oxygen atoms, but the values (in italics) shown on the surface are cumulative charges borne by the Pt slab. (a) Side view of the initial configuration. (b) Proton-transfer intermediate H−O−O generated at 0.15 ps. (c) Proton-transfer intermediate H−O−O at 0.44 ps. (d) One-end chemisorbed precursor H−O−O−Pt_n (adsorbed) at 0.53 ps. (e) H−O−O−Pt_n dissociation into H−O and O (adsorbed) at 0.73 ps. (f) Atop atomic adsorption at 0.89 ps.

Conclusions

- MD simulations are a very relevant and powerful « analysis » and « predicting » tool for providing insights into H2 production and conversion mechanisms
- Reactive MD is very powerful since availability of reactive and variable charge reaxFF potential family
- Matching experimental conditions is a condition for successful comparisons.

Thanks a lot for your attention